

Magic Wavelengths for Terahertz Clock Transitions

Xiaoji Zhou,* Xia Xu, Xuzong Chen, and Jingbiao Chen†

School of Electronics Engineering & Computer Science, Peking University, Beijing 100871, P. R. China

Magic wavelengths for laser trapping of boson isotopes of alkaline-earth Sr, Ca and Mg atoms are investigated while considering terahertz clock transitions between the $^3P_0, ^3P_1, ^3P_2$ metastable triplet states. Our calculation shows that magic wavelengths of trapping laser do exist. This result is important because those metastable states have already been used to realize accurate clocks in the terahertz frequency domain. Detailed discussions for magic wavelength for terahertz clock transitions are given in this paper.

PACS numbers: 0.6.20-f; 0.6.30-Ft; 32.80.Qk; 32.30.Bv.

I. INTRODUCTION

Frequency standards have achieved an unprecedented success in experimental demonstrating accuracies of 4×10^{-16} with a cesium microwave fountain clock [1] and 1.9×10^{-17} with an ion optical clock [2, 3]. For optical frequency standards based on neutral atoms, in order to effectively increase the interrogation time, Katori proposed to utilize optical lattice trap formed with a magic wavelength trapping laser [4, 5]. This clever technique greatly enhanced established high-accuracy optical frequency standard with neutral Sr atom to an accuracy of 1×10^{-16} [6–8]. Different optical clock schemes based on Ca [9], Yb [10, 11] atoms trapped with magic wavelength lasers have been proposed.

Optical trap with a far off-resonant laser is a very useful tool for the confinement of cold atoms. Nevertheless, for the precision of clock transitions in frequency standards, light shift due to trapping laser has to be avoided. Thus the wavelength of the trapping laser should be tuned to a region where the light shift for the clock transition is eliminated, that means the light shifts of the two clock transition states cancel each other. The wavelength λ is called magic wavelength [4, 5]. Recently, cesium primary frequency standard with atoms trapped in an optical lattice with a magic wavelength was suggested [12, 13], and possible magic wavelengths for clock transitions in aluminium and gallium atoms were also calculated [14].

In contrast to the above mentioned magic wavelengths for optical clock transitions and microwave clock transitions, here we investigate magic wavelengths for terahertz clock transitions. Absolute frequency standards in the terahertz domain with fine structure transition lines of the Mg and Ca metastable triplet states were first proposed in 1972 by Strumia [15]. After more than twenty years of continuing improvement, a frequency standard based on the $^3P_1 - ^3P_0$ Mg transition and thermal atoms in a beam has reached an uncertainty of 1×10^{-12} [16, 17]. However, these potential terahertz transitions for high-resolution clock references have never been experimentally investigated with laser cooled or laser trapped atoms.

In this paper, we present our most recent calculation

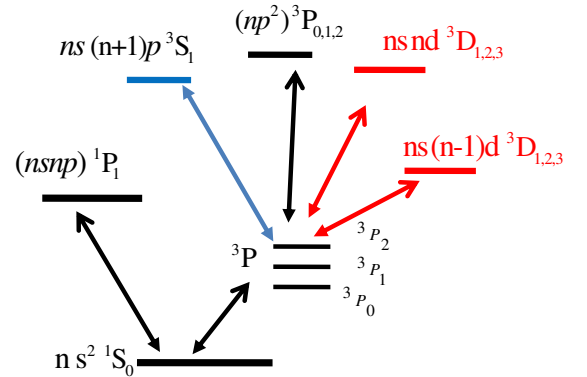


FIG. 1: (Color online) Simplified diagram of the lowest energy levels for alkaline-earth atoms and some possible laser couplings.

of trapping laser magic wavelengths for Sr, Ca and Mg atoms, considering different possible clock transitions between metastable triplet states 3P . Accurate terahertz clocks could then be built based on such atoms which are cooled and trapped in an optical lattice.

II. THEORETICAL DESCRIPTION

For alkaline-earth atoms, two valence electrons result in two series of atomic energy levels as the electron spins can be parallel (triplet states) or anti parallel (singlet state). The energy diagram can be simplified as shown in Fig. 1. The ground state is 1S_0 , and the lowest excited states $nsnp$ are 1P_1 and 3P_J which can be divided into three fine structure sublevels $^3P_2, ^3P_1, ^3P_0$. For the 3P_J state, transitions to higher states can be divided into three groups: $^3P_J - ^3S_1, ^3P_J - ^3P_J$ and $^3P_J - ^3D_J$.

By second-order perturbation theory, the energy shift $U_i(\omega, p, m_i)$ of atomic state $|i\rangle$ with energy E_i and Zeeman sublevel m_i , which is induced by a trapping laser field with frequency $\nu = \omega/2\pi$, polarization p , and irradiance intensity I can be expressed as $U_i(\omega, p, m_i) = -\alpha_i(\omega, p, m_i)I/2\epsilon_0 c$ with the

*Electronic address: xjzhou@pku.edu.cn

†Electronic address: jbchen@pku.edu.cn

induced polarizability α_i .

The polarizability can be calculated by summing up the contributions from all dipole interactions between the fine structure state $|i\rangle$ and $|k\rangle$ with the Einstein coefficient A_{Jki} (spontaneous emission rate for $E_k > E_i$), Zeeman sublevels m_i, m_k and transition frequency $\nu_{Jki} = \omega_{Jki}/2\pi$ [18, 33],

$$\alpha_i = 6\pi c^3 \epsilon_0 \sum_{k, m_k} \frac{A_{Jki}(2J_k + 1)}{\omega_{Jki}^2(\omega_{Jki}^2 - \omega^2)} \begin{pmatrix} J_i & 1 & J_k \\ m_i & p & -m_k \end{pmatrix}^2 \quad (1)$$

where

$$A_{Jki} = \frac{e^2}{4\pi\epsilon_0} \frac{4\omega_{Jki}^3}{3\hbar c^3} \frac{1}{2J_k + 1} |\langle \beta_k J_k || D || \beta_i J_i \rangle|^2 \quad (2)$$

Here e is the electron charge, $\hbar\omega_{Jki}$ is the energy difference between fine structure states $|k\rangle$ and $|i\rangle$, β denotes other quantum numbers of the state, and $\langle \beta_k J_k || D || \beta_i J_i \rangle$ is the dipole reduced matrix element. The expression in large parentheses in Eq.(1) denotes a $3J$ symbol which describes the selection rules and relative strength of the transition depending on the involved angular momenta J , the projection m , and the polarization p .

If we know ω_{Jki} and A_{Jki} in Eq.(1), we can get the polarizability α_i . However, typically the literature gives the total transition rate A_T from a given excited state to the fine structure manifold states below. So we need establish the relation

TABLE I: Sr element: Transition Wavenumbers (WN)(cm^{-1}) corresponding to ω_{Jki} , Einstein Coefficients for fine structure states $A_J(\times 10^6 s^{-1})$ and Total $A_T(\times 10^6 s^{-1})$ for fine structure states manifold, Correction Factors ζ . The Wavenumber data originate from [20].

UpperState	$5s^2 1S_0$			
	WN	A_J	ζ	A_T
$5s5p^1P_1$	21698.48	190.01	1.000	190.01 ^b
$5s6p^1P_1$	34098.44	1.87	1.000	1.87 ^d
$5s7p^1P_1$	38906.90	5.32	1.000	5.32 ^d
$5s8p^1P_1$	41172.15	14.9	1.000	14.9 ^a
$4d5p^1P_1$	41184.47	12	1.000	12 ^a
$5s9p^1P_1$	42462.36	11.6	1.000	11.6 ^a
$5s10p^1P_1$	43327.94	7.6	1.000	7.6 ^a
$5s11p^1P_1$	43938.26	4.88	1.000	4.88 ^a

UpperState	$5s5p^3P_0$			$5s5p^3P_1$			$5s5p^3P_2$			A_T
	WN	A_J	ζ	WN	A_J	ζ	WN	A_J	ζ	
$5s6s^3S_1$	14721.275	10.226	1.0828	14534.444	29.526	1.0421	14140.232	45.314	0.9596	85 ^c
$5s7s^3S_1$	23107.193	1.402	1.0517	22920.362	4.106	1.0264	22526.15	6.495	0.9743	12 ^e
$5s8s^3S_1$	26443.920	0.954	1.0450	26257.089	2.803	1.0230	25862.877	4.464	0.9776	8.22 ^a
$5s9s^3S_1$	28133.680	0.525	1.0422	27946.849	1.543	1.0216	27552.637	2.464	0.9790	4.53 ^a
$5s10s^3S_1$	29110.080	0.320	1.0408	28923.249	0.943	1.0208	28529.037	1.508	0.9797	2.77 ^a
$5p^2^3P_0$	—	0.000	—	20689.119	117.64	0.9803	—	0.000	—	120 ^e
$5p^2^3P_1$	21082.618	41.492	1.0373	20895.787	30.297	1.0099	20501.575	47.690	0.9538	120 ^e
$5p^2^3P_2$	—	0.000	—	21170.317	31.509	1.0503	20776.105	89.343	0.9927	120 ^e
$5s4d^3D_1$	3841.536	0.290	1.2660	3654.705	0.187	1.0901	3260.493	0.009	0.7740	0.412 ^f
$5s4d^3D_2$	—	0.000	—	3714.444	0.354	1.1444	3320.232	0.084	0.8174	0.412 ^f
$5s4d^3D_3$	—	0.000	—	—	0.000	—	3420.704	0.368	0.8938	0.412 ^f
$5s5d^3D_1$	20689.423	35.732	1.0544	20502.592	26.080	1.0261	20108.38	1.640	0.9681	61 ^g
$5s5d^3D_2$	—	0.000	—	20517.664	47.049	1.0284	20123.452	14.796	0.9702	61 ^g
$5s5d^3D_3$	—	0.000	—	—	0.000	—	20146.492	59.390	0.9736	61 ^g
$5s6d^3D_1$	25368.383	14.303	1.0457	25181.552	10.492	1.0228	24787.34	0.667	0.9755	24.62 ^f
$5s6d^3D_2$	—	0.000	—	25186.488	18.897	1.0234	24792.276	6.008	0.9761	24.62 ^f
$5s6d^3D_3$	—	0.000	—	—	0.000	—	24804.591	24.069	0.9776	24.62 ^f
$5s7d^3D_1$	27546.88	8.223	1.0424	27360.049	6.043	1.0213	26965.837	0.386	0.9778	14.2 ^a
$5s7d^3D_2$	—	0.000	—	27364.969	10.883	1.0219	26970.757	3.473	0.9783	14.2 ^a
$5s7d^3D_3$	—	0.000	—	—	0.000	—	26976.337	13.902	0.9790	14.2 ^a
$5s8d^3D_1$	28749.18	4.920	1.0407	28562.349	3.619	1.0206	28168.137	0.231	0.9789	8.51 ^a
$5s8d^3D_2$	—	0.000	—	28565.959	6.517	1.0210	28171.747	2.083	0.9793	8.51 ^a
$5s8d^3D_3$	—	0.000	—	—	0.000	—	28176.207	8.337	0.9797	8.51 ^a
$5s9d^3D_1$	29490.28	3.184	1.0400	29303.449	2.342	1.0203	28909.237	0.150	0.9797	5.51 ^a
$5s9d^3D_2$	—	0.000	—	29303.449	4.216	1.0203	28909.237	1.350	0.9797	5.51 ^a
$5s9d^3D_3$	—	0.000	—	—	0.000	—	28914.037	5.401	0.9802	5.51 ^a

^a [25], ^b [26], ^c [27], ^d [28], ^e [29], ^f [30], ^g [31].

TABLE II: Ca element: Transition wavenumbers (WN)(cm^{-1}) corresponding to ω_{Jki} , Einstein Coefficients for fine structure states $A_J(\times 10^6 s^{-1})$ and Total $A_T(\times 10^6 s^{-1})$ for fine structure states manifold, Correction Factors ζ . Besides the updated values listed in Ref. [33] for A_T , the others originate from [32].

$4s^2 1S_0$				
UpperState	WN	A_J	ζ	A_T
$4s4p^1P_1$	23652.304	218	1.000	218
$4s5p^1P_1$	36731.615	0.27	1.000	0.27
$4s6p^1P_1$	41679.008	16.7	1.000	16.7
$4snp^1P_1$	43933.477	30.1	1.000	30.1
$4s7p^1P_1$	45425.358	15.3	1.000	15.3
$4s8p^1P_1$	46479.813	6.1	1.000	6.1

$4s4p^3P_0$				$4s4p^3P_1$			$4s4p^3P_2$			
UpperState	WN	A_J	ζ	WN	A_J	ζ	WN	A_J	ζ	A_T
$4s5s^3S_1$	16381.594	9.855	1.0195	16329.432	29.278	1.0096	16223.552	47.845	0.9899	87 ^a
$4s6s^3S_1$	25316.340	3.488	1.0126	25264.178	10.397	1.0062	25158.298	17.110	0.9935	31
$4s7s^3S_1$	28822.866	1.573	1.0110	28770.704	4.692	1.0054	28664.824	7.733	0.9943	14
$4s8s^3S_1$	30580.783	1.033	1.0102	30528.621	3.083	1.0052	30422.741	5.084	0.9947	9.2
$4s9s^3S_1$	31590.382	0.606	1.0099	31538.220	1.809	1.0050	31432.340	2.985	0.9950	5.4
$4s10s^3S_1$	32224.147	0.370	1.0097	32171.985	1.105	1.0049	32066.105	1.824	0.9951	3.3
$4p^2^3P_0$	—	0.000	—	23207.480	179.046	0.9947	—	0.000	—	180
$4p^2^3P_1$	23306.907	60.474	1.0079	23254.745	45.045	1.0010	23148.865	74.033	0.9871	180
$4p^2^3P_2$	—	0.000	—	23341.495	45.563	1.0125	23235.615	134.784	0.9984	180
$3d^2^3P_0$	—	0.000	—	33314.030	110.231	1.0021	—	0.000	—	110
$3d^2^3P_1$	33379.722	36.971	1.0083	33327.560	27.594	1.0034	33221.680	45.540	0.9936	110
$3d^2^3P_2$	—	0.000	—	33353.459	27.662	1.0059	33247.579	82.178	0.9961	110
$4s4d^3D_1$	22590.296	48.981	1.0134	22538.134	36.471	1.0061	22432.254	2.396	0.9916	87
$4s4d^3D_2$	—	0.000	—	22541.804	65.687	1.0067	22435.924	21.580	0.9922	87
$4s4d^3D_3$	—	0.000	—	—	0.000	—	22441.506	86.400	0.9931	87
$4s5d^3D_1$	27585.101	20.786	1.0112	27532.939	15.498	1.0053	27427.059	1.021	0.9934	37
$4s5d^3D_2$	—	0.000	—	27534.653	27.905	1.0056	27428.773	9.192	0.9937	37
$4s5d^3D_3$	—	0.000	—	—	0.000	—	27431.444	36.782	0.9941	37
$4s6d^3D_1$	29891.172	13.472	1.0104	29839.010	10.049	1.0049	29733.130	0.663	0.9940	24
$4s6d^3D_2$	—	0.000	—	29840.356	18.094	1.0052	29734.476	5.965	0.9942	24
$4s6d^3D_3$	—	0.000	—	—	0.000	—	29736.431	23.868	0.9945	24
$4s7d^3D_1$	31144.072	8.417	1.0100	31091.910	6.279	1.0047	30986.030	0.414	0.9942	15
$4s7d^3D_2$	—	0.000	—	31093.586	11.306	1.0050	30987.706	3.729	0.9944	15
$4s7d^3D_3$	—	0.000	—	—	0.000	—	30990.116	14.922	0.9948	15
$4s8d^3D_1$	31878.324	4.318	1.0094	31826.162	3.221	1.0041	31720.282	0.213	0.9940	7.7
$4s8d^3D_2$	—	0.000	—	31829.944	5.803	1.0048	31724.064	1.915	0.9946	7.7
$4s8d^3D_3$	—	0.000	—	—	0.000	—	31729.298	7.663	0.9952	7.7
$4s3d^3D_1$	5177.459	0.502	1.0503	5125.297	0.365	1.0188	5019.417	0.023	0.9570	0.86 ^a
$4s3d^3D_2$	—	0.000	—	5139.197	0.663	1.0272	5033.317	0.207	0.9650	0.86 ^a
$4s3d^3D_3$	—	0.000	—	—	0.000	—	5055.057	0.841	0.9775	0.86 ^a

^a [33].

between A_{Tki} and A_{Jki} . We know A_{Tki} can be expressed as:

$$A_{Tki} = \frac{e^2}{4\pi\epsilon_0} \frac{4\omega_{Tki}^3}{3\hbar c^3} \frac{1}{2L_k + 1} |\langle \beta_k L_k || D || \beta_i L_i \rangle|^2 \quad (3)$$

Here $\hbar\omega_{Tki}$ is the energy difference between two fine structure manifold states $|k\rangle$ and $|i\rangle$. Using the formula:

$$\begin{aligned} \langle \beta_k J_k || D || \beta_i J_i \rangle &= (-1)^{L_k + S_k + J_i + 1} \delta_{S_k S_i} \sqrt{(2J_k + 1)(2J_i + 1)} \\ &\times \begin{Bmatrix} J_k & 1 & J_i \\ L_i & S_i & L_k \end{Bmatrix} \langle \beta_k L_k || D || \beta_i L_i \rangle \end{aligned} \quad (4)$$

and combining Eq.(2) and (3), we can get

$$A_{Jki} = A_{Tki} \times \zeta(\omega_{ki}) \widetilde{R}_{ki} \quad (5)$$

Here

$$\zeta(\omega_{ki}) = \omega_{Jki}^3 / \omega_{Tki}^3 \quad (6)$$

is the energy dependent correction [19], reflecting the alteration on the transition rate due to the effects such as the orbit-spin interaction and the spin-spin interaction which causes the fine structure splitting. And

$$\widetilde{R}_{ki} = (2L_k + 1)(2J_i + 1) \times \begin{Bmatrix} J_k & 1 & J_i \\ L_i & S_i & L_k \end{Bmatrix}^2 \quad (7)$$

gives the fraction of the coupling strength between an excited state $|k\rangle$ and a lower state $|i\rangle$. Since the total transition rate A_{Tki} is usually available in the literature, this geometric ratio tells

us how to scale the interaction for a particular fine structure state of interest.

To calculate the wavelength dependent polarizability, we combine Eq.(1) with Eq.(5), and use the known transition frequencies and spontaneous emission rates in the literature. This light polarizability is very sensitive to the Einstein coefficient. However, theoretical and experimental values of magic wavelength for the optical clock transition obtained in the past can be used to confirm our calculation.

In this paper, we use this method to calculate the light shift for the terahertz clock transition from 3P_0 to $^3P_1, m = 0$ levels, and from $^3P_1, m = 0$ to $^3P_2, m = 0$ levels for boson isotopes with the nuclear spin $I = 0$. After calculating magic wavelengths for Sr and Ca optical clock transitions and comparing them to the experimental values, we calculate the polarizability of terahertz transition with data collection mainly from Ref. [20, 25–32].

III. CALCULATION OF MAGIC WAVELENGTH

A. Strontium

Using the method above, for Strontium, we first calculate the magic wavelengths of two optical lattice clock transitions with the datas listed in Table I and compare the results with experimental values. Then, we calculate the crossing points for terahertz clock transitions where the difference of polarizability is zero. Table I shows Transition Wavenumbers, Einstein Coefficients and Correction Factors for the $5s^2\ ^1S_0$, $5s5p\ ^3P_0$, $5s5p\ ^3P_1$ and $5s5p\ ^3P_2$ states for Sr element. For Einstein Coefficient A_{Tki} , first we choose the available updated experimental values in Ref. [26, 28, 31], then we use updated theoretical data in Ref. [27, 30], and for the rest we mainly use theoretical values in Ref. [25].

According to our calculation, the crossing point for the 1S_0 to 3P_0 transition occurs at 813.1 nm, while the crossing point for the 1S_0 to $^3P_1(m_J = \pm 1)$ transition with linear polarized light takes place at 915.4 nm. Both of those results are in agreement with the experimental values of 813.428(1) nm [21–24] and 914(1) nm [27]. This confirms our calculation procedure.

Fig. 2 and Fig. 3 display the wavelength dependence of the atomic polarizability difference $\Delta\alpha$ for Sr with trapping laser wavelength around 400 nm and 1650 nm, respectively. The result is scaled by a factor of $1/(4\pi\epsilon_0 a_0^3)$ and the polarizability is given in atomic unit. In Fig.2, for linear polarized light, $\Delta\alpha$ between 3P_1 and 3P_0 and $\Delta\alpha$ between 3P_2 and 3P_1 are given in solid and dash dotted lines, respectively. In Fig.3, $\Delta\alpha$ between 3P_1 and 3P_0 for linear polarized light and $\Delta\alpha$ between 3P_2 and 3P_1 for circular polarized light are presented. The cross markers are the crossing points where $\Delta\alpha$ is zero. From Fig.2 and 3, we can know that the magic wavelength for 3P_0 to $^3P_1, m = 0$ with linear polarized light are 381.2 nm, 413.6 nm, 419.3 nm, 1714 nm and 3336 nm, while for $^3P_1, m = 0$ to $^3P_2, m = 0$ are 384.5 nm, 441.9 nm and 511.0 nm. On the other hand, for $m = 0$ and circular polarization of light, the magic wavelengths for 3P_0 to $^3P_1, m = 0$ transition are 511.8

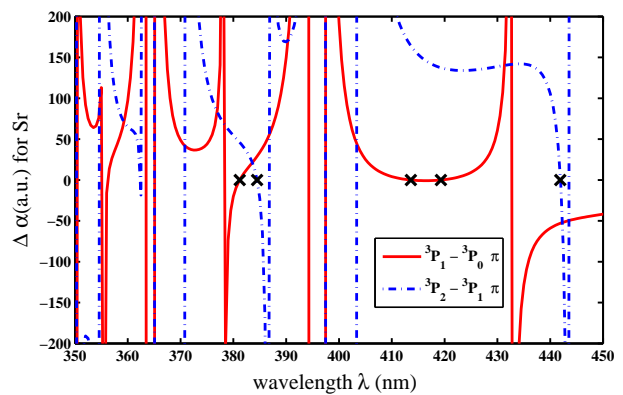


FIG. 2: (Color online) The wavelength dependence of the difference of atomic polarizability for Sr element around 400 nm.

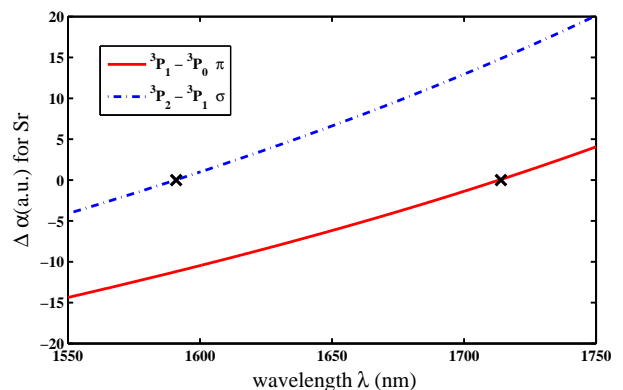


FIG. 3: (Color online) The wavelength dependence of the difference of atomic polarizability for Sr element around 1650 nm.

nm and 662.8 nm, while for $^3P_1, m = 0$ to $^3P_2, m = 0$, the magic wavelengths are 717.7 nm and 1591 nm.

B. Calcium

We calculate the polarizabilities using the data in Table II with the same method. Table II shows Transition Wavenumbers, Einstein Coefficients and Correction Factors for the $4s^2\ ^1S_0$, $4s4p\ ^3P_0$, $4s4p\ ^3P_1$ and $4s4p\ ^3P_2$ states for Ca. For Einstein Coefficient, we use the updated theoretical values according to Ref. [33], and others are from the data listed in Ref. [32]. In order to check the accuracy of our calculation and the data used, we get the magic wavelength 799.2 nm for the $^1S_0, m = 0$ to $^3P_1, m = 0$ optical transition with circularly polarized trapping light, which agrees well with the experimental value 800.8(22) nm [33].

The wavelength dependence of the atomic polarizability difference $\Delta\alpha$ around 350 nm and 1350 nm are shown with atomic unit in Fig.4 and 5, respectively. The crossing points where the $\Delta\alpha$ is zero are marked by cross. The magic wavelengths for linear polarization occur at 1361 nm and 2066 nm for clock transition $^3P_0 - ^3P_1$, while for the transition between

TABLE III: Mg element: Transition wavenumbers (WN)(cm^{-1}) corresponding to ω_{Jki} , Einstein Coefficients for fine structure states $A_J(\times 10^6 s^{-1})$ and Total $A_T(\times 10^6 s^{-1})$ for fine structure states manifold, Correction Factors ζ for Mg element. The Wavenumber and A_T data originate from [32].

$3s^2 1S_0$				
UpperState	WN	A_J	ζ	A_T
$3s3p^1P_1$	35051.264	491	1.000	491
$3s4p^1P_1$	49346.729	61.2	1.000	61.2
$3s5p^1P_1$	54706.536	16.0	1.000	16.0
$3s6p^1P_1$	57214.990	6.62	1.000	6.62
$3s7p^1P_1$	58580.230	3.28	1.000	3.28
$3s8p^1P_1$	59403.180	1.88	1.000	1.88

$3s3p^3P_0$				$3s3p^3P_1$			$3s3p^3P_2$			
UpperState	WN	A_J	ζ	WN	A_J	ζ	WN	A_J	ζ	A_T
$3s4s^3S_1$	19346.998	11.293	1.0063	19326.939	33.774	1.0032	19286.225	55.932	0.9968	101
$3s5s^3S_1$	30022.121	3.380	1.0041	30002.062	10.120	1.0020	29961.348	16.800	0.9980	30.3
$3s6s^3S_1$	34041.395	1.372	1.0036	34021.336	4.107	1.0018	33980.622	6.821	0.9982	12.3
$3p^2^3P_0$	—	0.000	—	35942.306	537.085	0.9983	—	0.000	—	538
$3p^2^3P_1$	35982.995	179.638	1.0017	35962.936	134.500	1.0000	35922.222	223.405	0.9966	538
$3p^2^3P_2$	—	0.000	—	36003.476	134.957	1.0034	35962.762	403.500	1.0000	538
$3s3d^3D_1$	26106.653	89.865	1.0047	26086.594	67.244	1.0024	26045.880	4.462	0.9977	161
$3s3d^3D_2$	—	0.000	—	26086.563	121.028	1.0023	26045.849	40.157	0.9977	161
$3s3d^3D_3$	—	0.000	—	—	0.000	—	26045.867	160.630	0.9977	161
$3s4d^3D_1$	32341.930	28.106	1.0038	32321.871	21.040	1.0019	32281.157	1.397	0.9981	50.4
$3s4d^3D_2$	—	0.000	—	32321.830	37.872	1.0019	32281.116	12.576	0.9981	50.4
$3s4d^3D_3$	—	0.000	—	—	0.000	—	32281.078	50.304	0.9981	50.4
$3s5d^3D_1$	35117.866	13.101	1.0035	35097.807	9.808	1.0017	35057.093	0.652	0.9983	23.5
$3s5d^3D_2$	—	0.000	—	35097.784	17.655	1.0017	35057.070	5.865	0.9983	23.5
$3s5d^3D_3$	—	0.000	—	—	0.000	—	35057.040	23.460	0.9983	23.5
$3s6d^3D_1$	36592.473	6.967	1.0033	36572.414	5.217	1.0017	36531.700	0.347	0.9983	12.5
$3s6d^3D_2$	—	0.000	—	36572.381	9.391	1.0017	36531.660	3.120	0.9983	12.5
$3s6d^3D_3$	—	0.000	—	—	0.000	—	36531.657	12.479	0.9983	12.5

level $^3P_1, m = 0$ and $^3P_2, m = 0$ at 312.2 nm, 316.2 nm, 325.4 nm, 344.0 nm and 393.4 nm.

The laser polarization have no effect on the polarizability for the ground state ($J = 0$) because the ac Stark shift is identical with any polarizations. It is also true for 3P_0 state. However, the influence of circular polarized laser light is worth study for other states. For $m = 0$, we can obtain the magic wavelengths for the 3P_0 to 3P_1 clock transition at 301.0 nm and 310.0 nm, while for 3P_1 to 3P_2 one finds 1318 nm and 2254 nm.

C. Magnesium

With the completion of the NIST database, the atomic polarizability of the Mg triplet states in the presence of linear and circular polarized light can also be calculated. Table III presents Transition Wavenumbers, Einstein Coefficients and Correction Factors for the $3s^2 1S_0$, $3s3p^3P_0$, $3s3p^3P_1$ and $3s3p^3P_2$ states for Mg element. Using the data presented in Table III, the magic wavelengths of 3P_0 to $^3P_1, m = 0$ transition with linear polarization are 335.6 nm and 399.5 nm. The magic wavelengths are 308.6 nm, 336.5 nm, 406.1 nm for the transition between $^3P_1, m = 0$ and $^3P_2, m = 0$.

For circular polarization of light, the magic wavelengths for the transition 3P_0 to $^3P_1, m = 0$ are 307.7 nm, 336.4 nm, 407.8 nm. However, we can not find any magic wavelength for cir-

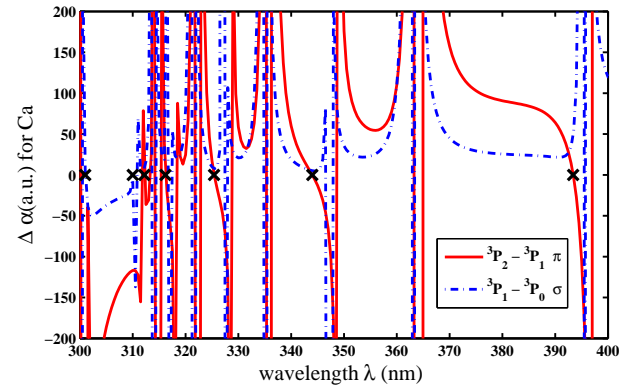


FIG. 4: (Color online) Wavelength dependence of the difference between excited state and ground state atomic polarizability around 350 nm for Ca element.

cular laser between level $^3P_1, m = 0$ and $^3P_2, m = 0$.

For Mg atoms, several optical transitions between the energy levels of terahertz clock transition states and other levels exist, such as 456.5 nm ($3s^2 1S - 3s3p^3P$), 383.6 nm ($3s3p^3P - 3s3d^3D$), 309.6 nm ($3s3p^3P - 3s4d^3D$), 333.2 nm ($3s3p^3P - 3s5s^3S$) and 517.4 nm ($3s3p^3P - 3s4s^3S$). Hence, not all the magic wavelengths are good enough for clock transition, because the slope of the light shift difference with the wavelength is too large (shown in the final table IV).

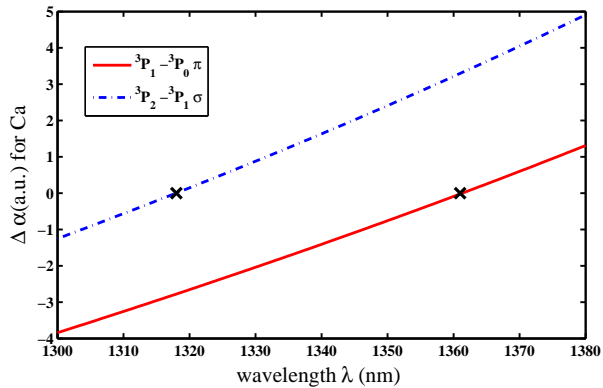


FIG. 5: (Color online) Wavelength dependence of the difference between excited state and ground state atomic polarizability around 1350 nm for Ca element.

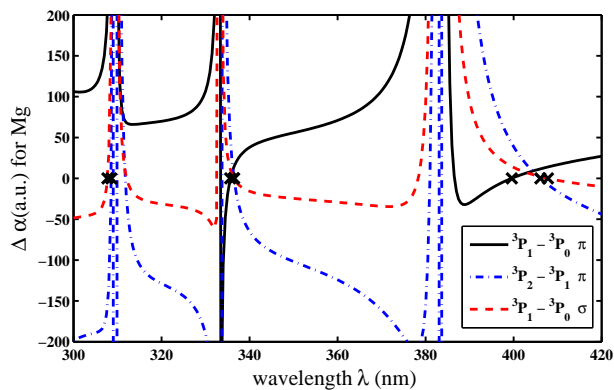


FIG. 6: (Color online) The wavelength dependence of the difference of atomic Polarizability around 400 nm for Mg element.

To some extent, a possible magic wavelength near 400 nm is shown in Fig. 6 with the atomic unit. In Fig. 6, $\Delta\alpha$ for ${}^3P_1-{}^3P_0$ transition and ${}^3P_2-{}^3P_1$ transition with different polarization are given. The cross markers reflect the crossing points where the atomic polarizability difference is zero.

IV. DISCUSSIONS AND CONCLUSIONS

In summary, we have calculated magic wavelengths for terahertz clock transitions for alkaline-earth atoms. The calculation results are presented in Table IV along with the slopes of the difference of polarizabilities at corresponding magic wavelengths. Depending on the calculation and the current laser development, we recommend 1714nm and 1591nm for Sr terahertz clock, 1361nm and 1318nm for Ca terahertz clock, 399.5nm and 407.8nm for Mg terahertz clock, because the difference of polarizabilities have small slopes at these magic wavelengths, where we ignore the effect of highly excited states and continuum states which can only make little contribution to the wavelength dependent polarizabilities at terahertz region.

TABLE IV: Magic wavelengths for terahertz region. L1 is the linear laser for the 3P_0 to 3P_1 clock transition while C1 is for the circular laser, L2 is the linear laser for the 3P_1 to 3P_2 clock transition while C2 is for the circular laser. κ is the slope of the shift difference of two level of clock transition levels at the corresponding trapping laser wavelength with unit Hz/nm , the sign denotes the direction of the change with the shift for the high level minus the lower level. The data are given in the reasonable experiment condition with input power 150 mW focused to a waist of 65 μm as the light intensity $1.1301 \times 10^3 W/cm^2$.

${}^3P_{0,1,2}$	Mg		Ca		Sr	
	λ (nm)	κ (Hz/nm)	λ (nm)	κ (Hz/nm)	λ (nm)	κ (Hz/nm)
L1	335.6	-1125	1361	-3.201	381.2	-615.7
	399.5	-103.5	2066	54.94	413.6	32.22
					419.3	-31.4377
					1714	-5.590
					3336	9.122
L2	308.6	-26574	312.2	8319	384.5	1792
	336.5	1905	316.2	5879	441.9	5759
	406.1	220.7	325.4	1641	511	1697.63
			344.0	542.9		
			393.4	1787		
C1	307.7	-3174	301.0	8610	511.8	252.8
	336.4	469.9	310.0	-4072	662.8	-1068
	407.8	54.76				
C2			1318	-3.365	717.7	2692
			2254	13.39	1591	-5.551

In this paper, we are only focusing on the study of possible magic wavelengths of trapping laser for these terahertz clock transitions of Sr, Ca and Mg atoms. These terahertz clock transitions were first proposed as early as 1972 [15], and recently have been proposed to be applied in active optical clock [34]. These clock transitions of alkaline-earth atoms correspond to a 0.6 THz to 11.8 THz frequency region. After the successful developments of microwave fountain frequency standards, optical clocks with trapped ions and optical lattice trapped neutral atoms, it is interesting to study clock transitions at terahertz wavelengths. The advantages and disadvantages of terahertz magic atomic clock will be discussed elsewhere. The wavelength range studied in this paper (from 500 μm to 25 μm) corresponding to THz frequency standards fills the gap between microwaves and optical waves.

We thank V. Thibault for critical reading our manuscript, and J. M. Li for his helpful discussions. We appreciate the anonymous referee for the useful suggestions. This work is partially supported by the state Key Development

Program for Basic Research of China (No.2005CB724503, 2006CB921401, 2006CB921402) and NSFC (No.10874008, 10934010, 60490280 and 10874009). This work is also supported by PKIP of CAS (KJCX2.YW.W10) and Open

Research Found of State Key Laboratory of Precision Spectroscopy (East China Normal University).

-
- [1] G. Santarelli, P. Laurent, P. Lemonde, A. Clairon, A. G. Mann, S. Chang, A. N. Luiten, and C. Salomon, *Phys. Rev. Lett.* **82**, 4619 (1999).
- [2] T. Schneider, E. Peik, and C. Tamm, *Phys. Rev. Lett.* **94**, 230801 (2005).
- [3] T. Rosenband, D. B. Hume, P. O. Schmidt, C. W. Chou, A. Brusch, L. Lorini, W. H. Oskay, R. E. Drullinger, T. M. Fortier, J. E. Stalnaker, S. A. Diddams, W. C. Swann, N. R. Newbury, W. M. Itano, D. J. Wineland, and J. C. Bergquist, *Science* **319**, 1808 (2008).
- [4] H. Katori, M. Takamoto, V. G. Pal'chikov, and V. D. Ovsianikov, *Phys. Rev. Lett.* **91**, 173005 (2003).
- [5] M. Takamoto, F. L. Hong, R. Higashi, and H. Katori, *Nature* **435**, 321 (2005).
- [6] G. K. Campbell, A. D. Ludlow, S. Blatt, J. W. Thomsen, M. J. Martin, M. H. G. de Miranda, T. Zelevinsky, M. M. Boyd, J. Ye, S. A. Diddams, T. P. Heavner, T. E. Parker, and S. R. Jefferts, *Metrologia* **45**, 539 (2008).
- [7] S. Blatt, A. D. Ludlow, G. K. Campbell, J. W. Thomsen, T. Zelevinsky, M. M. Boyd, and J. Ye, *Phys. Rev. Lett.* **100**, 140801 (2008).
- [8] A. D. Ludlow, T. Zelevinsky, G. K. Campbell, S. Blatt, M. M. Boyd, M. H. G. de Miranda, M. J. Martin, J. W. Thomsen, S. M. Foreman, J. Ye, T. M. Fortier, J. E. Stalnaker, S. A. Diddams, Y. Le Coq, Z. W. Barber, N. Poli, N. D. Lemke, K. M. Beck, and C. W. Oates, *Science* **319**, 1805-1808 (2008).
- [9] G. Wilpers, C. Oates, and L. Hollberg, *Applied Physics B: Lasers and Optics* **85**, 31 (2006).
- [10] Z. W. Barber, C. W. Hoyt, C. W. Oates, L. Hollberg, A. V. Taichenachev, and V. I. Yudin, *Phys. Rev. Lett.* **96**, 083002 (2006).
- [11] Z. W. Barber, J. E. Stalnaker, N. D. Lemke, N. Poli, C. W. Oates, T. M. Fortier, S. A. Diddams, L. Hollberg, C. W. Hoyt, A. V. Taichenachev and V. I. Yudin, *Phys. Rev. Lett.* **100**, 103002 (2008).
- [12] V. V. Flambaum, V. A. Dzuba, A. Derevianko, *Phys. Rev. Lett.* **101**, 220801 (2008).
- [13] X. J. Zhou, X. Z. Chen, J. B. Chen, Y. Q. Wang, J. M. Li, *Chin. Phys. Lett.* **26**, 090601 (2009).
- [14] K. Beloy, A. Derevianko, V. A. Dzuba, V. V. Flambaum, *Phys. Rev. Lett.* **102**, 120801 (2009).
- [15] F. Strumia, *Metrologia* **8**, 85 (1972).
- [16] A. Godone, and C. Novero, *Metrologia* **30**, 163 (1993).
- [17] A. Godone, C. Novero, P. Tavella, G. Brida, F. Levi, *IEEE Trans. Instrum. Meas.* **45**, 261 (1996).
- [18] R. Grimm, M. Weidemüller, and Y. B. Ovchinnikov, *Adv. At. Mol. Opt. Phys.* **42**, 95 (2000).
- [19] M. M. Boyd, Ph.D. Thesis (2007).
- [20] C. E. Moore, *Atomic Energy Levels: As Derived From the Analyses of Optical Spectra* (National Bureau of Standards, Washington D. C., 1971), Vol. 2, Page 190.
- [21] M. Takamoto, F.-L. Hong, R. Higashi, and H. Katori, *Nature* **435**, 321 (2005).
- [22] A. D. Ludlow, M. M. Boyd, T. Zelevinsky, S. M. Foreman, S. Blatt, M. Notcutt, T. Ido, and J. Ye, *Phys. Rev. Lett.* **96**, 033003 (2006).
- [23] A. Brusch, R. L. Targat, X. Baillard, M. Fouche, and P. Lemonde, *Phys. Rev. Lett.* **96**, 103003 (2006).
- [24] M. M. Boyd, A. D. Ludlow, S. Blatt, S. M. Foreman, T. Ido, T. Zelevinsky, and J. Ye, *Phys. Rev. Lett.* **98**, 083002 (2007).
- [25] H. G. C. Werij, C. H. Greene, C. E. Theodosiou, and A. Gallagher, *Phys. Rev. A* **46**, 1248 (1992).
- [26] M. Yasuda, T. Kishimoto, M. Takamoto, and H. Katori, *Phys. Rev. A* **73**, 011403 (2006).
- [27] T. Ido, and H. Katori, *Phys. Rev. Lett.* **91**, 053001 (2003).
- [28] W. H. Parkinson, E. M. Reeves, and F. S. Tomkins, *J. Phys.* **B9**, 157 (1976).
- [29] C. H. Corliss and W. R. Bozman, in *Experimental Transition Probabilities for Spectral Lines of 70 Elements*, edited by Editors Natl. Bur. Stand. (U.S.) Monogr. No. 53 (U.S. GPO, Washington, DC, 1962).
- [30] S. G. Porsev, A. D. Ludlow, M. M. Boyd, and J. Ye, *Phys. Rev. A* **78**, 032508 (2008).
- [31] H. J. Andra, H.-J. Plohn, W. Wittmann, A. Gaupp, J. O. Stoner Jr., and M. Gaillard, *J. Opt. Soc. Am.* **65**, 1410 (1975).
- [32] NIST Atomic Spectra Database, <http://physics.nist.gov/cgi-bin/AtData/main.asd>.
- [33] C. Degenhardt, H. Stoeck, U. Sterr, F. Riehle, and C. Lisdat, *Phys. Rev. A* **70**, 023414 (2004).
- [34] J. Chen, in *Frequency Standards and Metrology: Proceedings of the 7th Symposium*, edited by Maleki Lute (World Scientific Publishing Company, 2009).